J. Chem. Sci. Vol. 128, No. 9, September 2016, pp. 1345–1354. © Indian Academy of Sciences.
DOI 10.1007/s12039-016-1140-y

Carboxylic acid terminated, solution exfoliated graphite by organic acylation and its application in drug delivery

KOUSHIK BHOWMIK[a], AMRITA CHAKRAVARTY[a], U MANJU[b], GOUTAM DE[a,b,*] and ARNAB MUKHERJEE[a,*]

[a]Nano-Structured Materials Division, CSIR–Central Glass and Ceramic Research Institute, 196, Raja S C Mullick Road, Kolkata 700 032, India
[b]Advanced Materials Characterization Unit, CSIR-Central Glass and Ceramic Research Institute, 196, Raja S C Mullick Road, Kolkata 700 032, India
e-mail: gde@cgcri.res.in; arnabm@cgcri.res.in

MS received 6 April 2016; revised 15 June 2016; accepted 12 July 2016

Abstract. Graphite nanosheets are considered as a promising material for a range of applications from flexible electronics to functional nanodevices such as biosensors, intelligent coatings and drug delivery. Chemical functionalization of graphite nanosheets with organic/inorganic materials offers an alternative approach to control the electronic properties of graphene, which is a zero band gap semiconductor in pristine form. In this paper, we report the aromatic electrophilic substitution of solution exfoliated graphite nanosheets (SEGn). The highly conjugated π-electronic system of graphite nanosheets enable it to have an amphiphilic characteristic in aromatic substitution reactions. The substitution was achieved through Friedel–Crafts (FC) acylation reaction under mild conditions using succinic anhydride as acylating agent and anhydrous aluminum chloride as Lewis acid. Such reaction renders towards the carboxylic acid terminated graphite nanosheets (SEGn–FC) that usually requires harsh reaction conditions. The product thus obtained was characterized using various spectroscopic and microscopic techniques. Highly stable water-dispersed sodium salt of carboxylic acid terminated graphite nanosheets (SEGn–FC-Na) was also prepared. A comparative sheet-resistance measurements of SEGn, SEGn–FC and SEGn–FC-Na were also done. Finally, the anticancer drug doxorubicin (DOX) was loaded on water dispersible SEGn–FC-Na with a loading capacity of 0.266 mg mg^{-1} of SEGn–FC-Na and the release of DOX from this water-soluble DOX-loaded SEGn–FC-Na at two different temperatures was found to be strongly pH dependent.

Keywords. Solution exfoliated graphite; covalent functionalization; acid-terminated graphene; fridel-craft acylation; water dispersed graphite nanosheets; drug loading and release.

1. Introduction

Graphite nanosheets have attracted comprehensive research interest in carbon based nanoscience and technology.[1,2] Therefore, researchers are in a need of developing protocols for the mass production of graphene. One of the methods developed involves exfoliation of graphite to form stable dispersion in organic solvents or water by oxidizing graphite. But, at the same time measures to control defects and locally induced chemical changes occurring during such processes need to be found out. One such effective way may be direct covalent functionalization of graphite using mild reaction conditions. Such covalently functionalized graphite nanosheets have great promise in microelectronics,[3–5] photonics[5] as well as in biological applications.[6–8] Covalent chemical functionalization of exfoliated graphite nanosheets creates functional groups on their surface, which not only increases its dispersibility in water[9] but also creates a band gap for applications in microelectronics and photonics. In literature, a few reports are found on covalent functionalization of carbon nanotube.[10,11]

Covalent functionalization of graphite can be achieved through vigorous oxidation of graphitic flakes to obtain graphene oxide (GO).[12] However, such harsh uncontrolled functionalization of graphitic sheets, totally disrupts its in–plane π conjugation, leading to the formation of an insulator.[13] Additionally, GO has been recently described as a cytotoxic material.[14,15] Conversion of GO into reduced graphene oxide (RGO) is inadequate to restore the original graphene structure.[16] The RGO generally suffers from poor electrical conductance due to persisting oxidized defects. Recently,

*For correspondence

Pumera *et al.*, have used azobisisobutyronitrile (AIBN) to synthesize carboxylic acid terminated RGO.[17] An alternative route towards direct functionalization of graphite with groups that will not only lead to stable aqueous dispersions but will also be biocompatible is currently underway.

To maintain the extensive π conjugation and non-cytotoxicity in functionalized graphite nanosheets, direct covalent functionalization of exfoliated graphite nanosheets under mild conditions is believed to be a viable option. Due to the low chemical reactivity of graphite compared to fullerenes and carbon nanotubes, a few methods for its functionalization have been achieved. Diels–Alder cycloaddition, nitrene addition, arene cycloaddition and 1,3 dipolar cycloaddition on solution exfoliated graphite surface have been successfully performed by various groups.[4,18–20] Such chemical manipulation of graphite nanosheets is expected to stimulate the development of several new applications in many different fields. These applications include composites,[21,22] supercapacitors,[23] batteries,[24] fuel cells,[25] inks,[26] flexible touch screen displays,[27] intelligent coatings,[28] sensors,[29] photonics and optoelectronic devices.[30] However, none of the methods render towards an exclusive carboxylic acid terminated graphite nanosheets that can be potentially used for various biomedical and nano-composite applications.

Baek and co–workers have introduced a mild acylation method using a mixture of polyphosphoric acid (PPA) and phosphorus pentoxide (P_2O_5) on carbon nanotubes,[31,32] fullerenes[33] and on graphite[34,35] as a means of exfoliation. However; none of the methods seems to produce carboxylic acid terminated graphite nanosheets. The as-synthesized carboxylic acid functionalized graphite nanosheets can act as the potential points of departure for attachment of other functional groups,[36,37] amino acids,[38,39] and DNA[17] towards specific needs of various applications. Chen *et al.*, have synthesized water-dispersible graphene-butyric acid by Friedel-Craft acylation for electrochemical sensing application.[40] In this paper, we report the feasibility of a traditional Friedel–Crafts (FC) acylation on solution exfoliated graphite nanosheets (SEGn) to produce exclusively carboxylic acid terminated nanosheets with minimal defects. Further, we have synthesized water dispersible Na salt of the acid terminated graphite nanosheets (SEGn–FC-Na) for drug delivery application. The anticancer drug doxorubicin (DOX) was loaded onto this SEGn–FC-Na with sufficient loading capacity by π–π stacking interaction. Release of DOX from the SEGn–FC-Na was found to be pH dependent, which makes it a promising material for targeted delivery of anticancer drugs.

2. Experimental

2.1 *Materials*

The following chemicals were used as received. Graphite powder (<20 μm, synthetic) and doxorubicin hydrochloride were purchased from Aldrich. Succinic anhydride, anhydrous aluminium chloride ($AlCl_3$), ortho-Dichlorobenzene (ODCB), N-methyl-2-pyrolidone (NMP), sodium hydroxide (NaOH) and ethanol (EtOH) were supplied by Merck.

2.2 *Characterization*

The Friedel–Crafts acylation reaction on G and SEGn were monitored by Raman spectroscopy, Fourier transform infrared (FTIR) spectroscopy, X–Ray photoelectron spectroscopy (XPS), high–resolution transmission electron microscopy (HRTEM) and thermogravimetric analysis (TGA). Raman spectra were obtained using Renishaw InVia Reflex micro Raman spectrometer with excitation of argon ion (514 nm) laser. The laser power was kept sufficiently low to avoid heating of the samples and the spectra were collected with a resolution of 1 cm^{-1}. Multiple spectra (3–5) were obtained, normalized to the G band, and averaged to present a comprehensive overview of the material. FT–IR spectra of the samples were recorded using a Nicolet 380 FT–IR spectrometer by the KBr pellet method. XPS measurements were done on a PHI 5000 Versaprobe II XPS system with Al Kα source and a charge neutralizer at room temperature, maintaining a base pressure about 6×10^{-10} mbar and energy resolution of 0.6 eV. Low resolution survey scans and high resolution scans of C1s and O1s were taken. At least two separate locations were analyzed for each sample. HRTEM images were taken using a high resolution electron microscope JEOL JEM-2100F (FEG), operated at an accelerating voltage of 200 kV. TGA data was obtained using a Netzsch TG 209 F3 Tarsus thermal analyzer in argon atmosphere. Samples were degassed at 80°C for 15 min and then heated at 10°C/min to 600°C and held there for 20 min. Zeta potential of the aqueous dispersion of SEGn, SEGn–FC and SEGn–FC-Na were measured using a Nano Particle Analyzer SZ-100, Horiba. UV-Visible absorption spectra of the aqueous solutions containing DOX for monitoring the loading and release of the drug were recorded using a Cary 50, Varian Inc spectrometer.

2.3 *Preparation of SEGn*

SEGn was prepared according to the following procedure. 50 mg of microcrystalline graphite was subjected

to ultrasonic treatment for 1 h in 20 mL of ODCB. The resulting solution was centrifuged for 30 min at 4200 rpm to separate out the un-exfoliated graphitic bundles. The supernatant liquid contained dispersed exfoliated graphite in ODCB. This dispersion was directly used in the acylation reactions.

2.4 *Procedure of Friedel–Crafts acylation on SEGn*

In a typical experiment, anhydrous $AlCl_3$ (67 mg, 0.5 mmol) was charged into a three neck round bottom (RB) flask and dissolved in absolute EtOH under continuous purging of N_2 gas. As the $AlCl_3$ dissolves, the solution of succinic anhydride (50 mg, 0.5 mmol) in ethanol was added dropwise and stirred under N_2 atmosphere until a transparent solution appeared. To this solution, solution-exfoliated graphite (6 mg, 0.5 mmol, in ODCB) was added and the temperature was raised to 130°C. The reaction mixture was stirred continuously under refluxing condition for 24 h (Scheme 1). The resulting product was filtered using 0.22 μm PVDF membrane and the residue was washed successively with warm ethanol and chloroform to remove excess organic contents. The residue obtained was stirred with HCl (1 N) for 1 h and filtered through 0.22 μm PVDF membrane to remove excess $AlCl_3$. The carboxylic acid (–COOH) terminated SEGn obtained as residue was washed with excess water to remove HCl and dried overnight in vacuum at 80°C. The products obtained were designated as SEGn–FC.

2.5 *Synthesis of SEGn–FC-Na*

The SEGn–FC-Na was prepared by heating a dispersion of SEGn–FC (20 mg) in 1M NaOH (30 mL) overnight at 80°C under argon (Scheme 2). The contents were then diluted with water (100 mL), filtered through PVDF membrane (0.22 μm), and washed carefully with water.

2.6 *DOX loading on SEGn–FC-Na and release*

DOX was loaded onto SEGn–FC-Na following a procedure described in our earlier report.[41] In this process, 0.15 mg mL^{-1} of SEGn–FC-Na in water was sonicated with DOX solution of initial concentration 0.22 mg mL^{-1} at neutral pH (pH = 7) for 30 min. This solution was then stirred for 24 h in dark at room temperature (25°C). Finally, it was centrifuged at 11000 rpm for 30 min. The powder obtained was washed with water for several times to remove the unbound DOX and dried overnight under vacuum. The calibration curve for DOX was drawn with different known concentrations

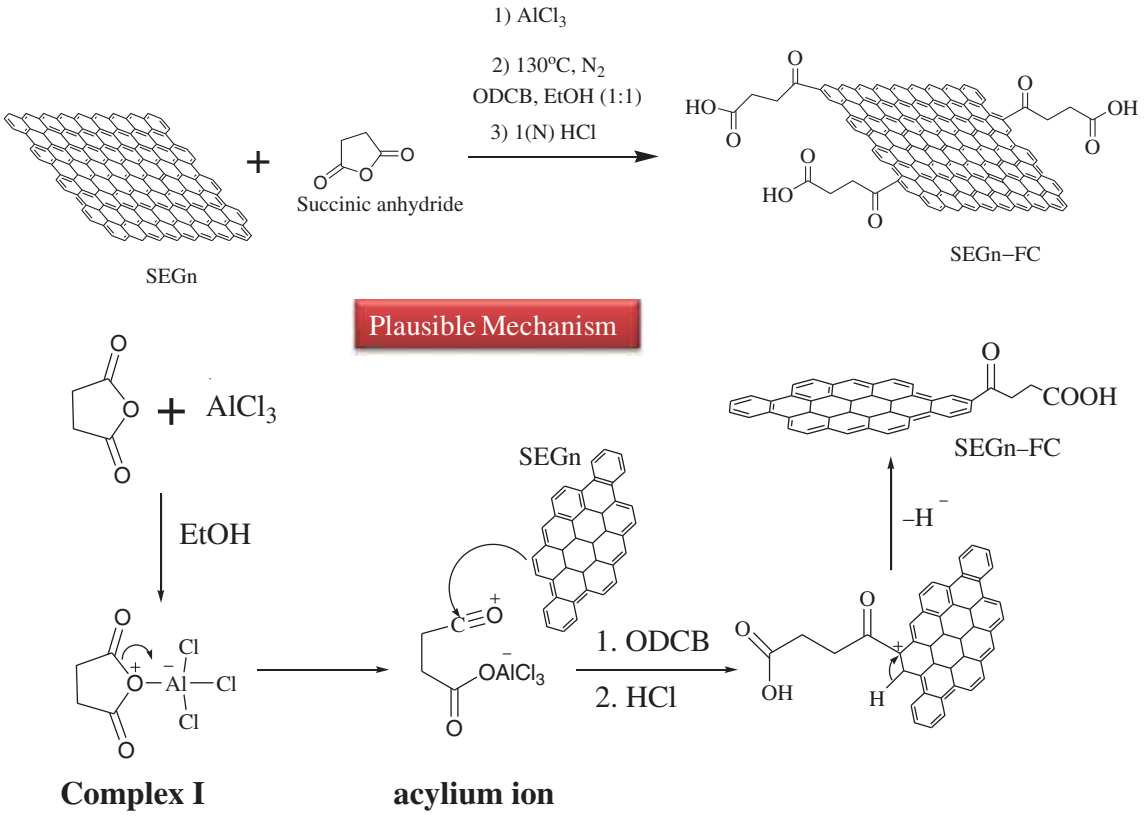

Scheme 1. Scheme of Friedel–Craft acylation on solution-exfoliated graphite nanosheets to synthesize carboxylic acid terminated graphite nanosheets.

by optical absorption spectral analysis at 480 nm. This calibration curve was used to determine the concentration of DOX. The DOX loading capacity for an initial concentration of 0.22 mg mL^{-1} of DOX and 0.15 mg mL^{-1} of SEGn–FC-Na was calculated using the following equation:

$$\text{Drug loading capacity} = (W_{\text{administered dose}} - W_{\text{residual dose}})/W_{\text{SEGn–FC-Na}}$$

Here, $W_{\text{administered dose}}$ indicates the initial weight of the drug used for loading, $W_{\text{residual dose}}$ indicates the residual weight of the drug present in the solution after loading onto SEGn–FC-Na and $W_{\text{SEGn–FC-Na}}$ indicates the weight of SEGn–FC-Na used for loading the drug. The DOX loaded SEGn–FC-Na composite was assigned as SEGn–FC-Na-DOX. The drug release behaviour of SEGn–FC-Na-DOX was monitored *in vitro* by dispersing the powder in phosphate buffer saline (PBS, pH 5.5 and 7.4 adjusted with phosphoric acid) under constant stirring at 25 and 37°C. The DOX dissolved supernatant solution was collected at different time intervals and analysed using UV-Vis spectroscopy.

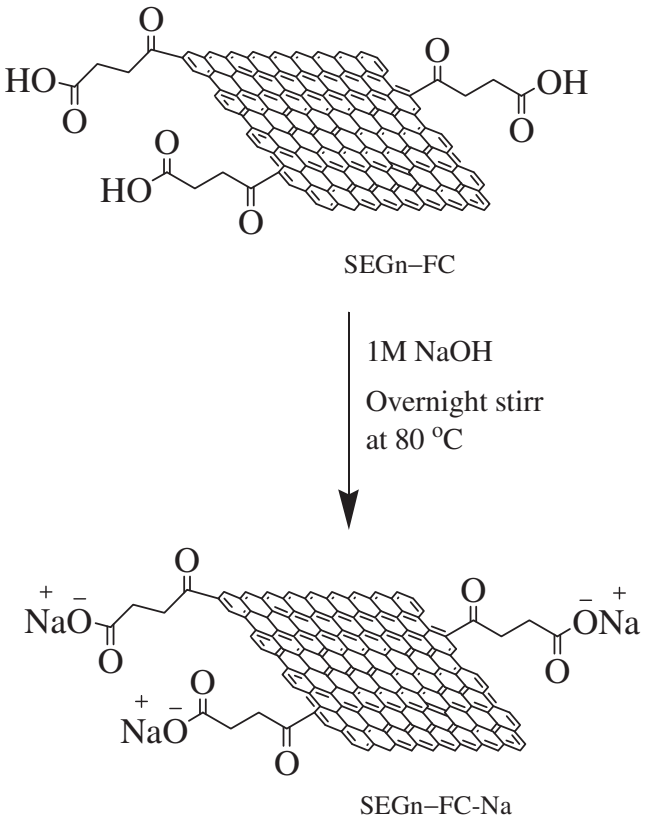

Scheme 2. Schematic representation for the synthesis of SEGn–FC-Na.

3. Results and Discussion

The microcrystalline graphite (G) was used to optimize the initial reaction conditions (reaction temperature and time) of FC acylation. The FC acylated G was designated as G–FC. The I_D/I_G values obtained from the Raman spectra were utilized to optimize the reaction conditions. Unfunctionalized G exhibits bands corresponding to the disorder mode (D band) at 1350 cm^{-1} and the tangential mode (the graphitic G band) at 1580 cm^{-1} (Figure S1 in Supplementary Information). The D band appears due to the A_{1g} breathing vibrations of the six membered sp^2 carbon rings and becomes Raman–active after the symmetry of the nearby lattice is reduced by the introduction of defects or functionality in graphitic material.[42] Higher the intensity ratio of the D and the G band (I_D/I_G), higher is the extent of covalent functionalization. The I_D/I_G values of G–FC obtained after FC acylation at various temperatures and time was compared and it was observed that the G–FC obtained from the reaction at 130°C for 72 h in ODCB/EtOH mixed solvent showed the highest I_D/I_G value of 0.3 (Table 1, entry 3) as shown in Supplementary Information (Figure S2 in Supplementary Information). Further, variations in the solvent (Table 1, entry 8), temperature (Table 1, entry 1, 2, 4 and 5) and reaction time (Table 1, entry 6 and 7) did not produce

Table 1. Optimization of FC-acylation at different temperature, solvent and time.

Entry	Reaction Temperature	Solvent	Reaction Time	I_D/I_G (G-FC)
1[a]	80°C	ODCB/EtOH	72 h	0.09
2[a]	110°C	ODCB/EtOH	72 h	0.14
3[a]	130°C	ODCB/EtOH	72 h	0.31
4[a]	150°C	ODCB/EtOH	72 h	0.17
5[a]	170°C	ODCB/EtOH	72 h	0.18
6[b]	130°C	ODCB/EtOH	24 h	0.19
7[b]	130°C	ODCB/EtOH	120 h	0.32
8[c]	130°C	NMP/EtOH	72 h	0.23

Raman spectra are provided in Supplementary Information. [a] Figure S2, [b] Figure S3 and [c] Figure S4.

any appreciable change in terms of the I_D/I_G values of G–FC obtained after FC acylation. Hence, entry 3, Table 1 represents the optimized reaction conditions. It is noteworthy here to mention that due to the negative inductive effect (-I) of electron withdrawing –Cl group on ODCB, it becomes highly deactivated towards aromatic electrophilic substitution reaction. Hence, ODCB can be safely used as a solvent for Friedel-Crafts acylation.[43,44] The enhanced reactivity of graphite as compared to ODCB is expected on theoretical grounds also.[45] Quantum-mechanical calculations show that the net loss in stabilization energy for the first step in electrophilic substitution is much lower in graphite or other polycyclic benzenoid hydrocarbon as compared to ODCB. This can be attributed to the fact that due to the fusion of more benzene rings, the positive charge generated in the transition state (T.S.) gets stabilized through delocalization, giving rise to a much stable transition state and lower activation energy for the reaction. As a control experiment, a reaction between ODCB and succinic anhydride with $AlCl_3$ as catalyst and in absence of graphite was performed. The reaction condition was kept same as mentioned in section 2.4. After 72 h, no solid product was obtained from the reaction. Similarly, the same reaction was performed in a non-aromatic solvent like NMP (Table 1, entry 8), where successful functionalization was achieved and it was confirmed by Raman spectroscopy studies ($I_D/I_G = 0.23$).

After optimization of the reaction conditions, the FC acylation was performed on SEGn and the product was designated as SEGn–FC. The schematic representation of the reaction is shown in Scheme 1. The succinic anhydride is not soluble in ethanol. When $AlCl_3$ was added to the solution, the complex I is formed which is soluble in ethanol and a clear solution was obtained. Then, the complex I is converted to the acylium ion. At high temperature, the π electrons of SEGn attack the acylium ion and form the compound II which undergoes H^+ rearrangement to give the final product SEGn–FC. The SEGn–FC was characterized by different spectroscopic and microscopic techniques.

Raman spectra of SEGn and SEGn–FC are presented in Figure 1. The unfunctionalized SEGn (Figure 1a) shows a very low I_D/I_G value of 0.08 that signifies an almost defect-free continuous sp^2 hybridized graphitic sheet. The enhanced D band ($I_D/I_G = 0.44$) of SEGn–FC observed upon functionalization, supports the covalent attachment of the succinic acid group onto the SEGn planes (Figure 1b).

Thermogravimetric analysis (TGA) profile of the degassed SEGn–FC was used to estimate the extent of functionalization (Figure 2). The starting SEGn showed

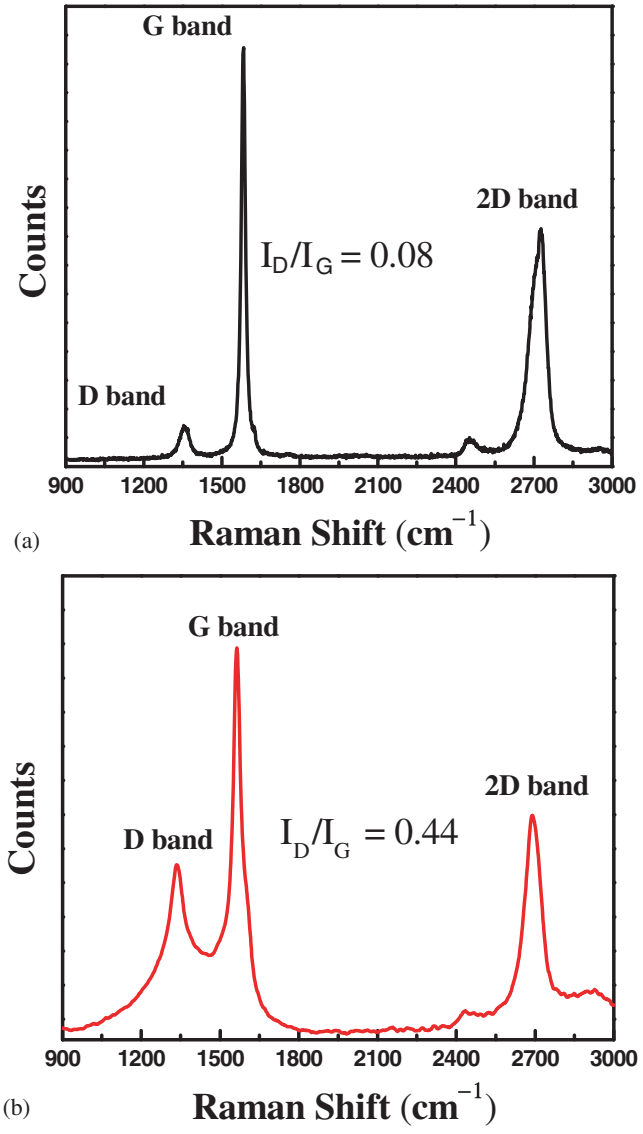

Figure 1. Raman spectra of (a) SEGn and (b) SEGn–FC.

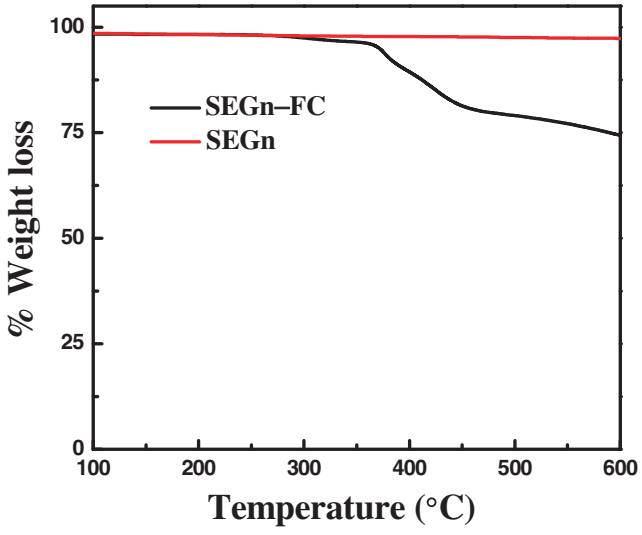

Figure 2. TGA weight loss patterns of SEGn and SEGn–FC in N_2 from 80 to 600°C.

no significant weight loss in TGA. However, around 350°C, the detachment of the functional groups from SEGn–FC leads to a weight loss of 20%, indicating that one functional group is present for approximately every 35 graphitic carbon atoms. This level of functionalization was found to be consistent with the enhancement of the D band observed *via* Raman spectroscopy and emphasized the efficiency of the functionalization process. The extent of functionalization was found to be comparable with previously reported other covalent functionalization on graphite.[46,47]

FTIR spectrum of SEGn shows peaks at 1580 and 1380 cm^{-1}. This can be attributed to C=C vibration of graphitic domain and C-OH bond vibrations, respectively (Figure 3a). But the FTIR Spectrum of SEGn–FC shows various new peaks (Figure 3b). The peaks at 1725 and 1630 cm^{-1} can be attributed to the $\nu_{C=O}$ of carboxylic acid group and $\nu_{C=O}$ of ketone, respectively. Apart from those, characteristic bands at 2930 and 2846 cm^{-1} for symmetric and antisymmetric stretching vibrations of $-CH_2$ confirm the covalent attachment of the succinic acid group to the planes of SEGn.

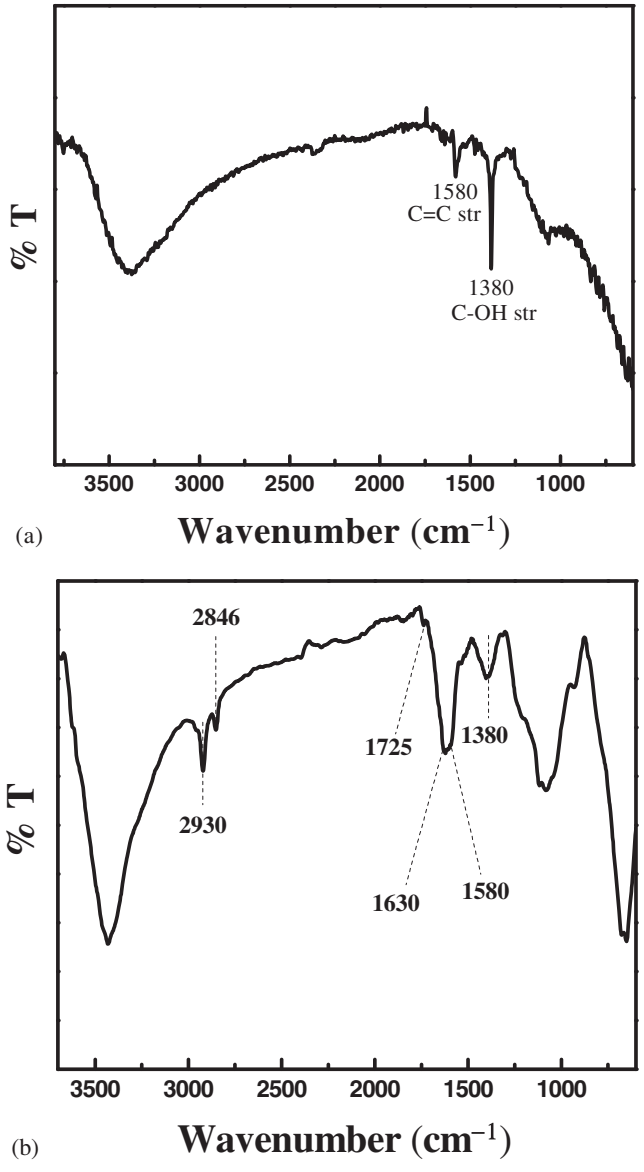

Figure 3. FTIR spectra of (a) SEGn and (b) SEGn–FC.

Both SEGn and SEGn–FC were also characterized using X–ray photoelectron spectroscopy (XPS). Voigt function was used for XPS peak deconvolution of the C1s and O1s peaks. The atomic percentages are based on the averaged peak areas of two different spots in the same sample and calculated using sensitivity factors 1.0 and 2.33 for carbon and oxygen, respectively. The survey scan of SEGn and SEGn–FC (Figure 4a) shows C1s and O1s features at 282.7 eV and 533 eV, respectively. In SEGn–FC, the intensity of O1s feature has increased significantly over SEGn. In SEGn, the atomic percentage of oxygen was found to be 4%, which significantly increased up to 13.7% in SEGn–FC. It can be attributed to the fact that in SEGn–FC, the graphitic surface got modified by oxygenated functional groups through FC acylation. The C1s high-resolution XPS (HRXPS) scan of SEGn–FC was fitted by deconvoluting five peaks (Figure 4b), each representing a separate carbon bond, accordingly, C=C (282.7 eV), C-C (283.4 eV), C–O (285 eV), C=O (287.05 eV), HOC=O (288.8 eV) and C–C shake-up (291.1 eV).[17,48–51] Whereas, the C1s envelop of SEGn shows three different types of carbon bonds, namely, C=C, C-O and C-C shake up (Figure S5 in Supplementary Information). The C-O peak in the starting SEGn originates from the presence of impurities or adsorbed moisture in the sample. In SEGn–FC, peaks corresponding to C-C, C=O and COOH arise due to the presence of covalently attached succinic acid group as shown in Scheme 1. Similarly, the O1s envelope in the O1s spectrum of SEGn–FC was fitted by deconvoluting three peaks (Figure 4c), each representing different oxygen functional groups, namely, C=O (531.8 eV),[52,53] COOH (533.4 eV),[52,53] and adsorbed water (535.4 eV).[54] The deconvoluted peak values of C1s and O1s in SEGn–FC confirm the successful FC acylation.

High-Resolution Transmission electron microscopy (HRTEM) image of SEGn–FC (Figure 5) clearly shows the graphite nanosheets. The interlayer distance of SEGn–FC was found to be 0.37 nm from the HRTEM image.

The SEGn–FC was treated with 1 M NaOH to form the Na-salt of SEGn–FC. The product was designated as SEGn–FC-Na (Scheme 2). It was observed that SEGn–FC-Na forms a stable dispersion in water after sonication for a few minutes (Figure 6a). The dispersion remains stable for a long period of time. As a control, the unfunctionalized SEGn was also treated with 1 M NaOH

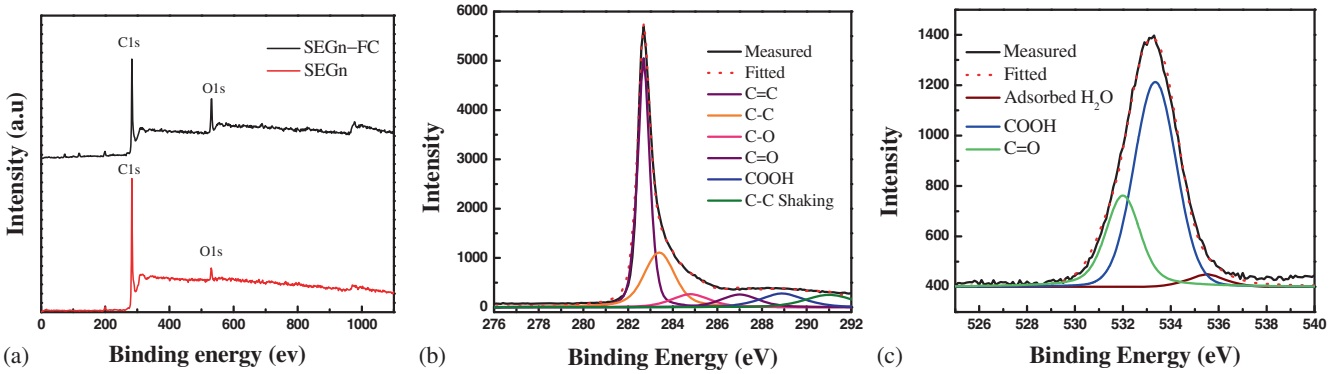

Figure 4. (a) Comparative XPS survey scans of SEGn and SEGn–FC; (b) deconvoluted C1s HRXPS of SEGn–FC; (c) deconvoluted O1s HRXPS of SEGn–FC.

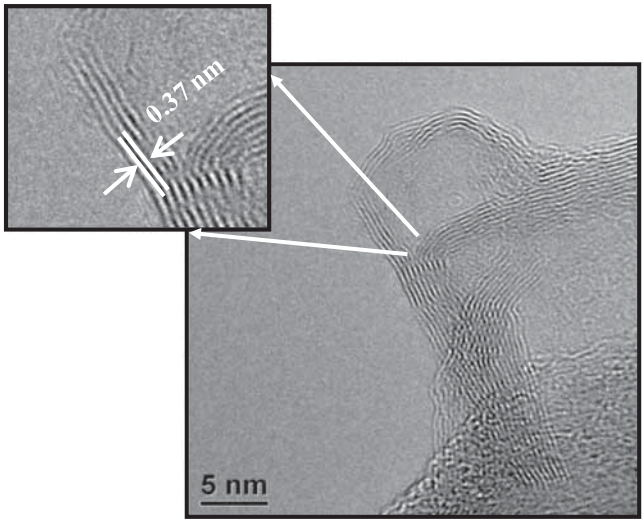

Figure 5. HRTEM image of SEGn–FC shows the interlayer spacing of around 0.37 nm.

following similar reaction conditions; it was found that the final product SEGn–Na was not dispersible in water (Figure 6b). Thus, this reaction and thereafter, the dispersion of the SEGn–FC-Na in water reconfirm the successful functionalization of SEGn with carboxylic acid functionality.

The SEGn–FC-Na was also characterized by FTIR and Raman spectroscopy. The FTIR spectrum shows characteristic peaks of carboxylate anion at 1560 and 1411 cm^{-1} (Figure S6a in SI). As the synthesis of SEGn–FC-Na is a secondary reaction on the carboxylic acid group of SEGn–FC, it does not affect the π electronic environment of the graphitic surface any further. Therefore, no significant change in the I_D/I_G value was observed in the Raman spectrum of SEGn–FC-Na (Figure S6b in SI). The zeta potential value for the aqueous dispersion of SEGn, SEGn–FC and SEGn–FC-Na at neutral pH was measured to verify their electrostatic stability in water (Figure 7a). The zeta potential of SEGn and SEGn–FC were observed −3.8 and −24.3 mV, respectively, which indicate lower stability of the water dispersion. But the zeta potential for SEGn–FC-Na was found to vary between −50 to −55 mV. The values of zeta potentials observed were found to be very close to the values for the zeta potential of graphene oxide (−60 to −70 mV).[55] ASTM (American Society for Testing and Materials) defines colloids with zeta potentials higher than 40 mV (negative or positive) to have "good stability". Therefore, the observed range of zeta potential for SEGn–FC-Na was found to be ideal for stabilizing conventional colloidal particles.[56] This aqueous dispersion of SEGn–FC-Na remained stable without any sign of coagulation for more than a month. We also measured the absorbance of the dispersion at different concentrations. We found a linear relationship (Figure 7b) between concentration (c) and absorbance (A) which proves that the dispersion is a non-aggregated homogeneous dispersion.

The sheet resistance of bulk films of SEGn, SEGn–FC and SEGn–FC-Na prepared by vacuum filtration using PVDF membrane (pore size: 0.22 μm) was determined. The electrical sheet resistance of the films on membrane was measured with a two point probe by making silver electrodes on the film surface.[12] Figure 8 shows the sheet resistance values of all the three samples. SEGn–FC has average sheet resistance value of 1.7 KΩ/sq, while that of the starting SEGn was measured to be 0.75 KΩ/sq. The increase in sheet resistance value can be attributed to the sp^3 defects that are formed during the functionalization of SEGn to SEGn–FC. It clearly supports our belief that due to functionalization under this condition, sp^3 defects were generated on the planes of SEGn. Much lower sheet resistance value of 0.31 kΩ/sq was measured for SEGn–FC-Na. It can be assumed that ionic conductance plays a major role for such a low value of sheet resistance in the case of SEGn–FC-Na.[9]

Finally, the anticancer drug DOX was loaded on SEGn–FC-Na by sonication followed by stirring (24 h). In case of SEGn–FC-Na-DOX, the DOX loading was

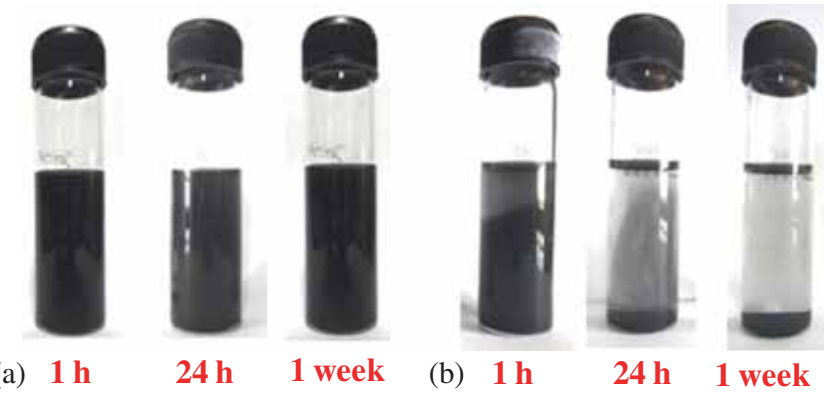

Figure 6. Images of, (a) stable dispersion of SEGn–FC-Na in water, and (b) unstable dispersion of SEGn-Na in water.

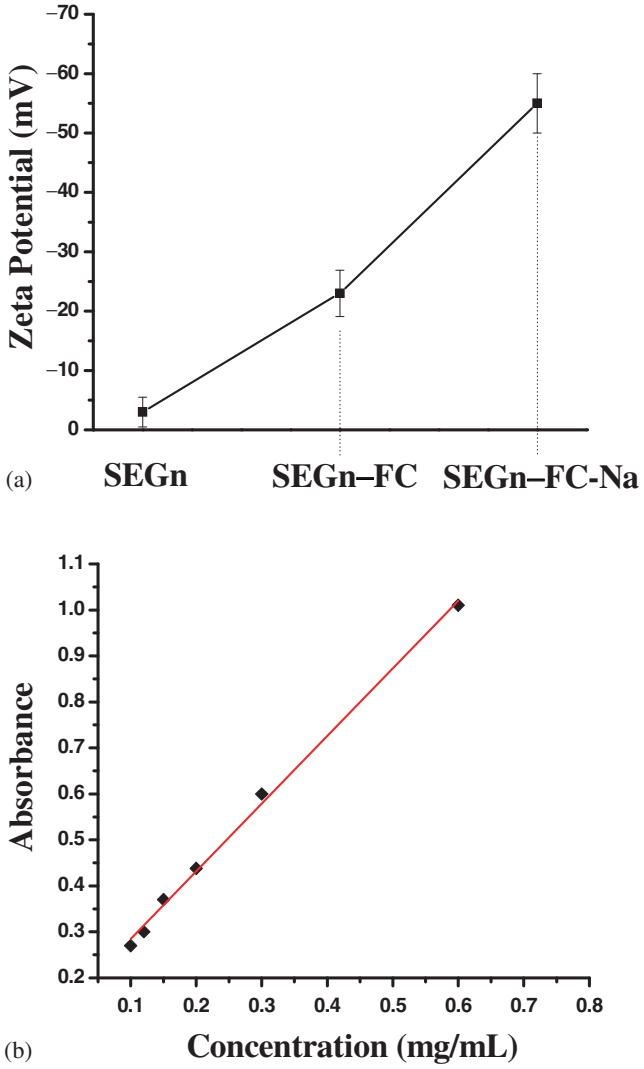

Figure 7. (a) Zeta potential of SEGn, SEGn–FC and SEGn–FC-Na; (b) concentration *vs* absorbance plot of SEGn–FC-Na dispersion in H_2O showing a linear relationship. Data points are joined for visual guide only.

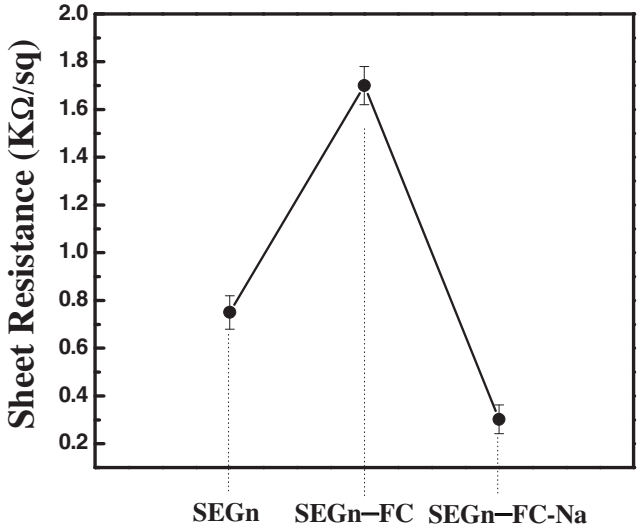

Figure 8. Graphical representation of the comparative sheet resistance values of SEGn, SEGn–FC and SEGn–FC-Na. The error range is shown with error bars. Data points are joined for visual guide only.

estimated from the UV-Vis spectra (Figure S7 in SI) and the calibration graph (Figure S8 in SI) and was found to be 0.266 mg mg^{-1} of SEGn–FC-Na. The evidence of successful loading of DOX in SEGn–FC-Na was observed from the FTIR spectra of SEGn–FC-Na-DOX and DOX as shown in Figure 9. Presence of peaks at 1204 and 1278 cm^{-1} for C-O stretching, prominent peak at 1417 cm^{-1} for C-C stretching and peak at 1725 cm^{-1} for C=O stretching of DOX[57,58] in the spectra of SEGn–FC-Na-DOX (Figure 9) confirmed the presence of DOX on the SEGn–FC-Na surface. Therefore, it is clear that DOX is loaded on SEGn–FC-Na, and it is expected to be attached to the system through π–π stacking interaction.

It is to be noted here that the SEGn–FC-Na has high solubility in water and the drug loading capacity in this case is also higher than the drug loading capacity of other common drug carrier materials such as liposomes and chitosans which have less than 0.1 mg mg^{-1} drug loading capacity.[59,60] The drug release study was performed at pH values of 5.5 and 7.4 at 37°C

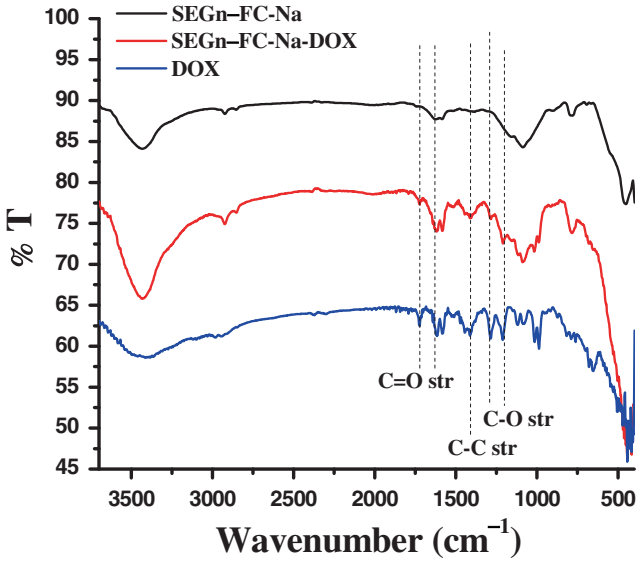

Figure 9. FTIR spectra of DOX, SEGn–FC-Na-DOX and SEGn–FC-Na.

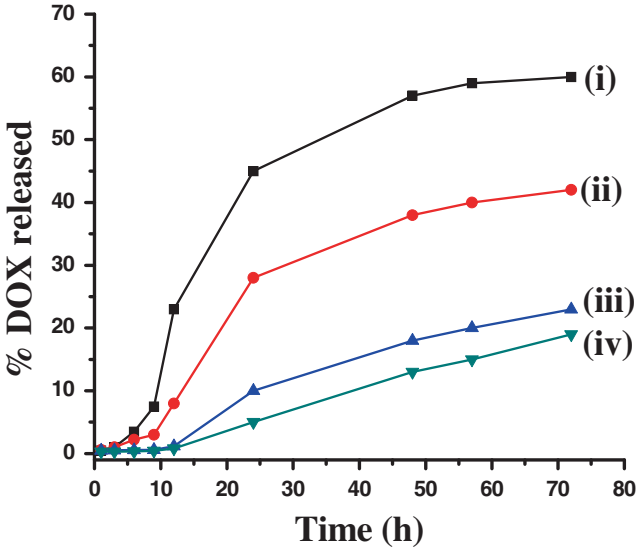

Figure 10. Release of DOX from SEGn–FC-Na-DOX: (i) pH 5.5 at 37°C, (ii) pH 5.5 at 25°C, (iii) pH 7.4 at 37°C and (iv) pH 7.4 at 25°C.

(*in vivo* physiological temperature) and 25°C (room temperature) as shown in Figure 10. The release of DOX was found to be very low under physiological pH (7.4) conditions with only about 22% and 19% of the bound DOX was released over 72 h at 37 and 25°C, respectively. However, under acidic pH (5.5) conditions, around 60 and 42% of DOX were released over the same period of time at 37 and 25°C, respectively. Thus, the pH sensitive and sustained release of DOX from the SEGn–FC-Na-DOX makes it a highly suitable and potential drug carrier for targeted anticancer drug delivery.

4. Conclusions

Traditional Friedel-Crafts acylation was successfully performed on solution exfoliated graphite nanosheets. The reaction was done under mild conditions with succinic anhydride as acylating agent and anhydrous aluminium chloride as Lewis acid. Apart from the spectroscopic and microscopic analysis, the formation of SEGn–FC was also confirmed by the synthesis of Na-salt of SEGn–FC. The Na salt of SEGn–FC formed a stable suspension in water. The comparative sheet resistance values confirm the successful functionalization of the solution exfoliated graphite nanosheets and their subsequent salt formation. Finally, the anticancer drug doxorubicin was loaded on water dispersible SEGn–FC-Na with a loading capacity of 0.266 mg mg^{-1} and its release was studied at pH 5.5 and 7.4 over 72 h at 25 and 37°C. The low cost and efficient drug release up to 60% in pH 5.5 at 37°C over 72 h makes it a potential drug carrier for applications in the field of targeted drug delivery.

Supplementary Information (SI)

Raman spectrum of microcrystalline graphite; Raman spectra of the G-FC obtained from reactions performed at various temperatures, time and solvent; XPS analysis of SEGn; FTIR and Raman spectra of SEGn–FC-Na; UV-Vis spectra of DOX solution before and after loading; and calibration curve of DOX solution are provided in Supplementary Information which is available at www.ias.ac.in/chemsci.

Acknowledgements

KB and AC thank the CSIR, India for providing fellowships.

References

1. Dreyer D R, Park S, Bielawski C W and Ruoff R S 2010 *Chem. Soc. Rev.* **39** 228
2. Geim A K 2009 *Science* **324** 1530
3. Li B and Cao H 2011 *J. Mater. Chem.* **21** 3346
4. Sarkar S, Bekyarova E, Niyogi S and Haddon R C 2011 *J. Am. Chem. Soc.* **133** 3324
5. Liu L and Yan M 2011 *J. Mater. Chem.* **21** 3273
6. Hong B J, Compton O C, An Z, Eryazici I and Nguyen S T 2012 *ACS Nano* **6** 63
7. Zhang Q, Li W, Kong T, Su R and Li N 2013 *Carbon* **51** 164
8. Singh S K, Singh M K, Kulkarni P P, Sonkar V K, Gracio J J A and Dash D 2012 *ACS Nano* **6** 2731
9. Mukherjee A, Kang J H, Kuznetsov O, Sun Y, Thaner R, Bratt A S, Lomeda J R, Kelly K F and Billups W E 2011 *Chem. Mater.* **23** 9

10. Panchakarla L S and Govindaraj A 2008 *J. Chem. Sci.* **120** 607
11. Kakade B, Patil S, Sathe B, Gokhale S and Pillai V 2008 *J. Chem. Sci.* **120** 599
12. Bhowmik K, Pramanik S, Medda S K and De G 2012 *J. Mater. Chem.* **22** 24690
13. Eda G, Mattevi C, Yamaguchi H, Kim H and Chhowalla M 2009 *J. Phys. Chem. C* **113** 15768
14. Wojtoniszak M, Chen X, Kalenczuk R J and Wajda A 2012 *Colloids Surf., B* **89** 79
15. Yang K, Wan J, Zhang S, Zhang Y, Tong–Lee S and Liu Z 2010 *ACS Nano* **5** 516
16. Boukhvalov D W and Katsnelson M J 2008 *J. Am. Chem. Soc.* **130** 10697
17. Bonanni A, Chua C K and Pumera M 2014 *Chem. Eur. J.* **20** 217
18. Strom T A, Dillon E P, Hamilton C E and Barron A R 2010 *Chem. Commun.* **46** 4097
19. Meier M S, Wang G W, Haddon R C, Brock C P, Lloyd M A and Selegue J P 1998 *J. Am. Chem. Soc.* **120** 2337
20. Georgakilas V, Bourlinos A B, Zboril R, Steriotis T A, Dallas P, Stuboscd A K and Trapalis C 2010 *Chem. Commun.* **46** 1766
21. Stankovich S, Dikin D A, Dommett H B, Kohlhaas K M, Zimney E J, Stach E A, Piner R D, Nguyen S T and Ruoff R S 2006 *Nature* **442** 282
22. Bai S and Shen X 2012 *RSC Adv.* **2** 64
23. Wu Q, Xu Y, Yao Z, Liu A and Shi G 2010 *ACS Nano* **4** 1963
24. Yoo E, Kim J, Hosono E, Zhou H, Kudo T and Honma I 2008 *Nano Lett.* **8** 2277
25. Qu L, Liu Y, Baek J B and Dai L 2010 *ACS Nano.* **4** 1321
26. Lucechinger N A, Athanassious E K and Stark W J 2008 *Nanotechnology* **19** 445201
27. Wang S, Ang P K, Wang Z, Tang A L L, Thong J T L and Loh K P 2010 *Nano Lett.* **10** 92
28. Lee V, Whittaker L, Jaye C, Baroudi K M, Fischer D A and Banerjee S 2009 *Chem. Mater.* **21** 3905
29. Mohanty H N and Berry V 2008 *Nano Lett.* **8** 4469
30. Bonaccorso F, Sun Z, Hassan T and Ferrari C 2010 *Nature Photon.* **4** 611
31. Jeon Y, Choi H J, Bae S Y, Chang D W and Baek J B 2011 *J. Mater. Chem.* **21** 7820
32. Lee H J, Han S W, Kwon Y D, Tan L S and Baek J B 2008 *Carbon* **46** 1850
33. Lim D H, Lyons C B, Tan L S and Baek J B 2008 *J. Phys. Chem. C* **112** 12188
34. Choi E K, Jeon I Y, Bae S Y, Lee H J, Shin H S, Dai L and Baek J B 2010 *Chem. Commun.* **46** 6320
35. Chua C K and Pumera M 2012 *Chem. Asian J.* **7** 1009
36. Shan C, Wang L, Han D, Li F, Zhang Q, Zhang X and Niu L 2013 *Thin Solid Films* **534** 572
37. Liu H, Kuila T, Kim N H, Kud B C and Lee J H 2013 *J. Mater. Chem. A* **13** 739
38. Shan C S, Yang H F, Han D X, Zhang Q X, Ivaska A and Niu L 2009 *Langmuir* **25** 12030
39. Gao J, Liu F, Liu Y, Ma N, Wang Z and Zhang X 2010 *Chem. Mater.* **22** 2213
40. Chen H C, Chen Y H, Chen S L, Chern Y T, Tsai R Y and Hua M Y 2013 *Biosens. Bioelectron.* **46** 84
41. Chakravarty A, Bhowmik K, De G and Mukherjee A 2015 *New J. Chem.* **39** 2451
42. Ferrari A C, Meyer J C, Scardaci V, Casiraghi C, Lazzeri M, Mauri F, Piscane S, Jiang D, Novoselov K S, Roth S and Geim A K 2006 *Phys. Rev. Lett.* **97** 187401
43. Aribert N, Camy S, Lucchese Y P, Condoret J S and Cognet P 2010 *Int. J. Chem. Reactor Eng.* **8** A53
44. Boroujeni K P 2010 *Turk. J. Chem.* **34** 621
45. Wade L G 2013 In *Organic Chemistry*, Indian Edition, 6th edn. (New Delhi: Pearson Education) p. 748
46. Mukherjee A, Combs R, Chattopadhyay J, Abmayr D W, Engel P S and Billups W E 2008 *Chem. Mater.* **20** 7339
47. Zhong X, Jin J, Li S, Niu Z, Hu W, Li R and Ma J 2010 *Chem. Commun.* **46** 7340
48. Li M, Boggs M, Beebe T P and Huang C P 2008 *Carbon* **46** 466
49. Luong J H T, Hrapovic S, Liu Y L, Yang D Q, Sacher E and Wang D S 2005 *J. Phys. Chem. B* **109** 1400
50. Xing Y C, Li L, Chusuei C C and Hull R V 2005 *Langmuir* **21** 4185
51. Kovtyukhova N I, Mallouk T E, Pan L and Dickey E C 2003 *J. Am. Chem. Soc.* **125** 9761
52. Jiang Z, Yu X, Jiang Z, Menga Y and Shi Y 2009 *J. Mater. Chem.* **19** 6720
53. Okpalugo T I T, Papakonstantinou P, Murphy H, McLaughlin J and Brown N M D 2005 *Carbon* **43** 153
54. Nevskaia D M and Martín-Aranda R M 2003 *Catal. Lett.* **87** 143
55. Si Y and Samulski E T 2008 *Nano Lett.* **8** 1679
56. *Zeta Potential of Colloids in Water and Waste Water* 1985 ASTM Standard D 4187-82, American Society for Testing and Materials
57. Kemp W 1991 In *Organic Spectroscopy* 3rd edn. (New York: Palgrave)
58. Wu S, Zhao X, Li Y, Du Q, Sun J, Wang Y, Wang X, Xia Y, Wang Z and Xia L 2013 *Materials* **6** 2026
59. Sun W T, Zhang N, Li A G, Zou W W and Xu W F 2008 *Int. J. Pharm.* **353** 243
60. Lim E K, Sajomsang W, Choi Y, Jang E, Lee H, Kang B, Kim E, Haam S, Suh J S, Chung S J and Huh Y M 2013 *Nanoscale Res. Lett.* **8** 467